The FASEB Journal • Research Communication

Regulation of human protease-activated receptor 1 (*hPar1*) gene expression in breast cancer by estrogen

Zaidoun Salah,*[,1] Beatrice Uziely,*[,1] Mohammad Jaber,*[,1] Miriam Maoz,* Irit Cohen,* Tamar Hamburger,* Bella Maly,[†] Tamar Peretz,* and Rachel Bar-Shavit*[,2]

*Sharett Institute of Oncology and [†]Department of Oncology, Hadassah-Hebrew University Hospital, Jerusalem, Israel

ABSTRACT **A pivotal role is attributed to the estrogen-receptor (ER) pathway in mediating the effect of estrogen in breast cancer progression. Yet the precise mechanisms of cancer development by estrogen remain poorly understood. Advancing tumor categorization a step forward, and identifying cellular gene fingerprints to accompany histopathological assessment may provide targets for therapy as well as vehicles for evaluating the response to treatment. We report here that in breast carcinoma, estrogen may induce tumor development by eliciting protease-activated receptor-1 (PAR_1) gene expression. Induction of PAR_1 was shown by electrophoretic mobility shift assay, luciferase reporter gene driven by the $hPar_1$ promoter, and chromatin-immunoprecipitation analyses. Functional estrogen regulation of *hPar1* in breast cancer was demonstrated by an endothelial tube-forming network. Notably, tissue-microarray analyses from an established cohort of women diagnosed with invasive breast carcinoma exhibited a significantly shorter disease-free ($P=0.006$) and overall ($P=0.02$) survival of patients that were positive for ER and PAR_1, compared to ER-positive but PAR_1-negative patients. We propose that estrogen transcriptionally regulates $hPar_1$, culminating in an aggressive gene imprint in breast cancer. While ER^+ patients are traditionally treated with hormone therapy, the presence of PAR_1 identifies a group of patients that requires additional treatment, such as anti-PAR_1 biological vehicles or chemotherapy.—Salah, Z., Uziely, B., Jaber, M., Maoz, M., Cohen, I., Hamburger, T., Maly, B., Peretz, T., B.-S, R. Regulation of human protease-activated receptor 1 (*hPar1*) gene expression in breast cancer by estrogen. *FASEB J.* 26, 2031–2042 (2012). www.fasebj.org**

Key Words: thrombin · tumor · ERE · tissue microarray

Abbreviations: BAEC, bovine aortic endothelial cell; ChIP, chromatin immunoprecipitation; CM, conditioned medium; DFS, disease-free survival; E_2, estrogen; EGFR, epidermal growth factor receptor; EMSA, electrophoretic mobility shift assay; ER, estrogen receptor; ERE, estrogen response element; GPCR, G-protein coupled receptor; LUC, luciferase; NE, nuclear extract; OS, overall survival; PAR_1, protease-activated receptor 1; PR, progesterone receptor; TNBC, triple-negative breast cancer; WT, wild type.

Breast cancer comprises a heterogeneous group of diseases categorized into 3 major subtypes (1, 2). Among these are tumors that possess estrogen receptors (ERs) and progesterone receptors (PRs), breast tissues that overexpress HER2, and triple-negative breast cancer (TNBC) tissues. While the first 2 may well respond to endocrine therapy or biologically targeted anti-HER2 vehicles, TNBC is considered the most aggressive subtype. Furthermore, TNBC lacks any detectable molecular signature and is the most poorly understood. Consequently, a major challenge in breast cancer is to identify molecular targets to possibly expand current categories and assist in determining treatment.

While the human mammary gland is highly dependent on estrogen (E_2) for normal growth and maintenance (3–5), ligation of E_2 to ER, a nuclear transcription factor, is the driving force in breast cancer progression (6). E_2-bound ER serves as a potent transcription factor for the induction of novel genes downstream that are important for normal cellular function and tumor growth, independent of proliferation (7–10). These downstream genes may consequently become central targets in breast cancer therapy (11). The main dogma for transcriptional regulation by E_2 involves the following steps: binding of E_2 to ER to initiate receptor phosphorylation, receptor dimerization, and association of the ligand-ER complex with binding motifs in the promoter of target genes. Concomitantly, E_2-bound ER favors the recruitment of coactivators that enhance its transcriptional activity. In fact, the coregulators serve as a fine-tuning device for receptor transcriptional activity. Several coregulators have been implicated in cancer, most notably AIB1 (SRC3), which is overexpressed in the majority (two-thirds) of all breast cancers.

The ER signaling pathway in breast cancer is thought to be regulated also outside the nucleus, initiated at the cell membrane *via* crosstalk with receptor tyrosine kinases, including epidermal growth factor receptor

[1] These authors contributed equally to this work.

[2] Correspondence: Sharett Institute of Oncology, Hadassah-Hebrew University Hospital, P.O. Box 12000, Jerusalem 91120, Israel. E-mail: rachel.bar-shavit@ekmd.huji.ac.il

doi: 10.1096/fj.11-194704

(EGFR or HER2/Neu) and insulin-like growth factor receptor IR (12–14). This might be a mode of ER activation in the E_2-resistance pathway. These receptor kinases activate signaling pathways, culminating in the phosphorylation of ER as well as its coactivators and corepressors at multiple sites and influencing their specific final function (15).

Protease-activated receptor 1 (PAR_1), a G-protein-coupled receptor (GPCR), is the first and prototype member of the mammalian PAR family that comprises 4 genes (16, 17). While a well-known classical observation points to a tight link between hyperactivation of the coagulation system and cancer malignancies, the molecular mechanism that governs procoagulant tumor progression remains poorly defined (18–20). There is correlation between levels of *hPar1* expression and breast cancer progression in both clinically obtained biopsy specimens and a wide spectrum of differentially metastatic cell lines (21–24). PAR_1 is associated with breast cancer malignancy. Its expression correlates with the aggressiveness of human breast carcinoma cell lines, and there is increased expression of the *hPar1* gene and protein in human breast tumors when compared with corresponding normal tissues (21). Mammary gland tumors produced by MCF7 breast carcinoma cells, genetically engineered to overexpress either wild-type (WT) full-length *hPar1* cDNA or a superactive form of *hPar1*, were considerably larger and more vascularized when compared with the truncated form devoid of the cytoplasmic tail or mock-injected cell-producing tumors (25). This observation indicates that PAR_1 is capable of eliciting mammary tumors in a tight association with PAR_1-driven signaling. Consequently, we wondered whether there is hormonal regulation of *hPar1* gene expression in the context of breast tissues.

In the present study, we investigated E_2 regulation of PAR_1 in breast carcinoma and established its functional effect. A shorter disease-free survival (DFS; $P=0.006$), as well as overall survival (OS; $P=0.026$), were observed in ER^+ and $PAR_1{}^+$ women compared with ER^+ but $PAR_1{}^-$ patients from a tissue microarray of an established cohort of individuals with invasive breast carcinoma. This outcome identifies PAR_1 as part of an aggressive gene imprint. Collectively, our data suggest transcriptional regulation of *hPar1* by E_2-bound ER. Noticeably, the presence of PAR_1 may contribute to decisions on treatment. While ER^+ women receive hormone treatment, the presence of PAR_1 identifies a group that may also need either anti-PAR_1 biological vehicles (currently emerging in the market) or chemotherapy.

MATERIALS AND METHODS

Cells

MCF-7 and T47D cells (American Type Culture Collection, Manassas, VA, USA) were grown in RPMI 1640 supplemented with 10% fetal calf serum, L-glutamine, penicillin, and streptomycin. Steroid-depleted cell culture medium was RPMI 1640 phenol red-free medium supplemented with 10% charcoal-stripped fetal bovine serum. Bovine aortic endothelial cells (BAECs) were cultured in DMEM (with glucose, 1 mg/ml) supplemented with 10% calf serum and bFGF (26).

RNA extraction and RT-PCR

Total RNA was prepared using TRI reagent (Molecular Research Center, Cincinnati, OH, USA) as described by the manufacturer. PCR primers were as follows: *hPar1*, upstream 5′-GCCAGAATCAAAAGCAACAA-3′ and downstream 5′-GAGATGAATGCAGGAAGTTGTTT-3′; GAPDH, upstream 5′-CCACCCATGGCAAATTCCATGGCA-3′ and downstream GADPH: 5′-TCTAGACGGCAGGTCAGGTCCACC-3′.

PCR products were separated on a 1.5% agarose gel stained with ethidium bromide and visualized under ultraviolet light.

Activation of PAR_1

PAR_1 was activated by the TFLLRNPNDK peptide, a selective PAR_1 agonist, or thrombin (1 U/ml).

Transfection and luciferase (LUC) expression assay

MCF-7 cells, grown for 48 h in steroid-depleted cell culture medium to 60–80% confluency, were transfected with 2 μg of the *hPar1* promoter fragment plasmid DNA Poluc-HTR/-4.1 (F1; kindly provided by Dr. Marschall S. Runge, University of North Carolina at Chapel Hill, Chapel Hill, NC, USA) or empty expression plasmid (2 μg), and CMVβgal (0.3 μg) in FuGene-6 transfection reagent (Roche Diagnostics Co., Indianapolis, IN, USA). After 48 h, the cells were either treated for the indicated periods of time with E_2 (Sigma-Aldrich, St. Louis, MO, USA) or not, and then lysed in 0.1 ml of lysis buffer (Promega, Madison, WI). Luciferase activity was measured as described previously (27).

Electrophoretic mobility shift assay (EMSA)

Nuclear extracts (NEs) were prepared as described previously (27, 28). Complementary oligonucleotide probes were synthesized (Metabion, Martinsreid, Germany) for the *hPar1* putative estrogen-response element (ERE) sites according to GenBank accession number U63331: P1, 5′-agatgcgcaggTGACCcccg at site −2081; P2, 5′-ccctGTCActacatcataa-3′ at site −2150; and P5, 5′-ccctGTCActacatcataa-3′ (R) at site −2654. The C consensus sequence ERE is 5′-cagGTCAtcaTGACCtg-3′. Underscored sequences indicate the seed sequence of ERE (uppercase letters). Lowercase letters indicate a mutation inserted into the sequence. For competition experiments, 1- to 100-fold of unlabeled double-stranded oligonucleotide was added 15 min prior to incubation. The oligos for P3 and P4 are as follows: P3, 5′-ttagcgaaaactTGAaCtttt-3′; P4, 5′-gcggccgtCTcGACCctcct-3′. Mutants for each of the oligos are as follows: mutant P1, 5′-agatgcgcaggtACCccg-3′; mutant P2, 5′-tta tgatgtagTtACaggg-3′; mutant P3, 5′-ttagcg aaaactTtAACttt-3′; mutant P4, 5′-gcggccgtCTcGtCCctcct-3′; mutant P5, 5′-gaagctgttcagTtACtCac-3′.

Chromatin immunoprecipitation (ChIP) and PCR analysis

MCF-7 cells were grown for 48 h in serum-free starvation medium and then either left untreated or treated with E_2 (10^{-8} M) for 2 h. ChIP was performed as described previously (27, 29). Following treatment, MCF-7 cells were fixed with

formaldehyde (to a final concentration of 1%) at room temperature for 10 min to cross-link histone proteins to DNA. Glycine was then added (to a final concentration of 0.125 M) to the plates to quench formaldehyde. Soluble chromatin was isolated and sonicated. Samples were then centrifuged at 13,000 rpm for 10 min, and the supernatant was collected. For the immunoprecipitation step, 10 μg of antibodies, prebound to protein A/G Sepharose beads, was added to 500 μl of the purified chromatin sample and incubated overnight at 4°C. Ab-immunocomplexed DNA was then recovered by phenol/chloroform extraction, ethanol precipitation, and resuspension in TE. PCR primer sets were designed to overlap and span the ERE binding sites of the *hPar1* promoter. ERE primer set I: forward, 5′-actgtcgacgtctccacacatc-3′, and reverse, 5′-tgtaatccccgcactttaggag-3′; set II: forward, 5′-tgtaatccccgcactttaggag-3′, and reverse, 5′-ccactgtcgacgtc tccacatccc-3′. These primers were first evaluated using the *Par1*-Luc construct as a DNA template. Semiquantitative PCR was then performed using the Titanium *Taq*PCR kit (Clontech Laboratories, Palo Alto, CA, USA). Amplification was carried out for 35 cycles (28 cycles for unprecipitated chromatin input lanes) with denaturation at 94°C for 1 min, annealing at 58°C for 30 s, and extension at 72°C for 1 min. PCR products were separated on a 2% agarose gel.

ELISA

Quantification of the levels of VEGF secreted by *hPar1* cells was carried out by ELISA (Quantikine/human VEGF; R&D Systems, Minneapolis, MN), performed according to the manufacturer's instructions with anti-VEGF neutralizing Abs C20 (Santa Cruz Biotechnology, Santa Cruz, CA, USA).

Calcium flux assay

Intracellular Ca^{+2} flux was measured in MCF-7 cells labeled with fura-2AM (a cell-permeable acetoxymethyl ester form of Fura-2; eBioscience, San Diego, CA, USA) by the ratio of fluorescence excitation intensity at 340/380 nm on a Fluro Scan Ascent SL (Thermo Electron Corp., Waltham, MA, USA).

Three-dimensional (3D) tube-forming assay

The assay was performed as described previously (24). Briefly, type I collagen matrix gel was obtained by simultaneously raising the pH and ionic strength of the collagen solution. Collagen was then used to coat 24-well plates (0.3 ml/well). After polymerization of the collagen at 37°C for 0.5 h, BAECs (2×10^4 cells/0.5 ml/well) were added to each well. Collagen solution (0.4 ml) was carefully placed on top of the cells. After the gel was formed, 0.4 ml of conditioned medium (CM) from the different treatment was added and replaced with fresh medium every other day. Tube formation and alignment of BAECs were visualized by phase microscopy at d 8–10. The morphometric analysis used to evaluate tube formation was performed as follows. Briefly, every well in a given plate (per treatment) was independently evaluated by 2 investigators (M.J. and R.B.). Discrepancies were resolved by simultaneous reexamination of the wells by both investigators using a double-headed microscope. The microscope was calibrated with a micrometer slide before each measurement. Ten fused cells/field were selected, and ≥50 fused cells/treatment case were assessed. Four microscopic fields were screened. Data are reported as means ± SD, and *P* values were determined by χ^2 test; values of $P < 0.05$ were considered significant. The data are representative of 4 independent experiments performed in triplicate.

Tissue microarray construction, immunostaining, and statistics

Formalin-fixed, paraffin-embedded breast carcinoma tissues from 299 nonselected patients with invasive breast carcinoma (220 ductal, 33 lobular, 13 ductal + lobular, 7 medullary, 3 mucinous, 9 DCIS, and 14 DCIS + microinvasion) were obtained from the Department of Pathology, Hadassah Medical Center (Jerusalem, Israel). The use of these specimens and data in research was approved by the Ethics Committee of the Hadassah Medical Center. Sections (5 μm) stained with hematoxylin and eosin (H&E) were obtained to confirm the diagnosis and to identify representative areas of the specimen. From these defined areas, 3 tissue cores with a diameter of 0.6 mm were taken with a manual tissue arrayer MTA-1 (Beecher Instruments, Sun Prairie, WI, USA) as described previously (30, 31). From each specimen, 3 tissue cores with a diameter of 0.6 mm were taken from the different regions of the tumor and arrayed in triplicate on a recipient paraffin block (28). Sections of 5 μm of the recipient blocks were cut and placed on charged polylysine-coated slides. Immunodetection of PAR_1 was done as described previously (25) with minor modifications. Briefly, sections of the tissue array blocks were deparaffinized and rehydrated. Tissue was then incubated in 3% H_2O_2, denatured by boiling (3 min) in a microwave oven in citrate buffer (0.01 M, pH 6.0), and blocked with 10% goat serum in PBS. Sections were incubated with polyclonal anti-PAR_1 antibody raised against a peptide (NH_2-CLLRNPNDKYEPFWED-COOH) representing an internal sequence downstream of the PAR_1 cleavage site, for activation. We also used polyclonal rabbit anti-PAR_1 antibody directed against a synthetic peptide (NH_2-KSSPLQKQLPAFISC-COOH) corresponding to an internal sequence of PAR_1 cleavage site, downstream of the above-mentioned peptide. The antibody was diluted 1:100 in 10% goat serum in PBS. Control slides were incubated with 10% goat serum alone. Color was developed using the Zymed AEC substrate kit (Zymed Laboratories, Burlingame, CA, USA) for 10 min, followed by counterstaining with Mayer's hematoxylin. For immunodetection of ERa and PR, monoclonal antibodies NCL-L-ER 6F11 and NCL-PGR-312, respectively, were used (Novocastra, Newcastle upon Tyne, UK). Slides were visualized with a Zeiss axioscope microscope (Carl Zeiss, Oberkochen, Germany) and manually read by an expert pathologist (B.M.). Tumors were considered positive for ER/PR if nuclear staining was seen in ≥10% of the tumor cells. To define a tumor as PAR_1^+, staining of ≥25% of the tissue was considered positive on the basis of an initial overview of the cases to improve signal-to-noise ratios. We also tested additional, even stricter, cutoffs (*i.e.*, ≥50%, ≥75%) of tumor cells staining for PAR_1. χ^2 tests were done to study the PAR_1 expression in ER^+ immunohistochemical results, using SPSS software (SPSS Inc., Chicago, IL, USA).

RESULTS

The *hPar₁* gene regulatory region contains 5 consensus EREs

A bioinformatic search of the regulatory region of *hPar₁* (U63331, 4.1 kb in size; ref. 27) revealed 5 candidates for EREs. The sequences of these putative ERE are −1853 to −1870, 5′-agatgcgcaggTGACCcccg-3′; −2078 to −2096, 5′-ccctGTCActacatcataa-3′ (R); −2159 to −2169, 5′-ttagcgaaaacTGAaCttt-3′; −2281 to −2300, 5′-aggagGGTCgagacggccgc-3′ (R); −2351 to −2368, 5′-ccctGTCActacatcataa-3′, shown in **Fig. 1*A***. To exam-

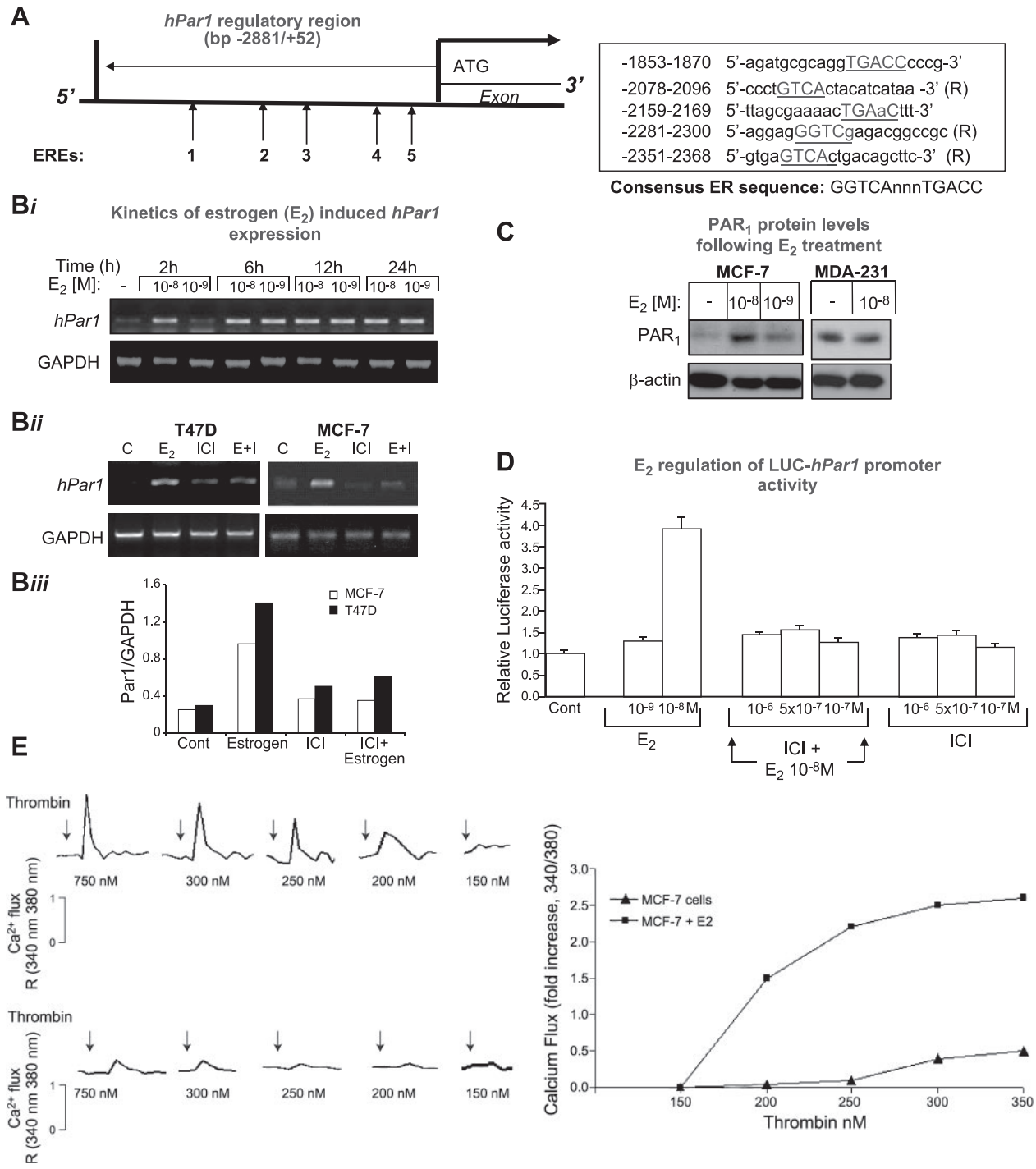

Figure 1. E_2 treatment induces *hPar1* promoter activity and increases its expression. *A*) Scheme of *hPar1* regulatory region and the potential ERE sequences identified. *Bi*) Kinetics of E_2-treated MCF-7 cells. Two concentrations (10^{-8} and 10^{-9} M) of E_2 were applied for various time periods as indicated, followed by RNA isolation and RT-PCR analysis for levels of PAR_1. While a marked enhancement in PAR_1 level is seen by 2 h of 10^{-8} M treatment and remains up to 24 h, no effect is seen by 2 h at 10^{-9} M. At this concentration, an elevated level of PAR_1 is observed after 4 h treatment and continuously up to 24 h. Similar data were obtained when T47D cells were analyzed (data not shown). Data are representative of ≥5 experiments. *Bii*) Specificity of E_2 treatment on PAR_1 levels. RT-PCR analysis of *hPar1* performed on RNA isolated from MCF-7 and T47D cells before and after E_2 treatment (2 h, 10^{-8} M) shows induced *hPar1* expression (as demonstrated in *Bi*). This induction was specifically inhibited in the presence of ICI182,780, a potent E_2 inhibitor, while application of ICI alone had no effect on PAR_1 levels. Data are representative of 3 experiments. *Biii*) Histogram represents band intensity after normalization with the GAPDH housekeeping gene. *C*) PAR_1 protein levels following E_2 treatment: Western blot analysis of MCF-7 and MDA-231 cells before and after E_2.Level of cell lysate loading is verified by β-actin levels. An increase in PAR_1 levels in MCF-7 cells is obtained at 10^{-8} M E_2. In contrast, no effect on PAR_1 levels is observed when MDA-231 cells lacking ER were similarly treated. Data are representative of ≥3 experiments. *D*) E_2 regulation of *hPar1*-LUC-promoter activity. MCF-7 cells were transiently transfected with *hPar1*-LUC reporter

(*continued on next page*)

ine whether E_2 modulates *hPar1* expression, we used semiquantitative reverse-transcription PCR, Western blot, and *hPar1*-driven LUC promoter activity to estimate *hPar1* mRNA expression in ER^+ breast carcinoma cells. As shown in Fig. 1*Bi*, a marked increase in *hPar1* RNA levels in MCF-7 cells was obtained following 2 and 6 h of E_2 treatment with 10^{-8} and 10^{-9} M, respectively. This high level was observed up to 24 h at both concentrations. The specificity for E_2 regulation was demonstrated in 2 cell lines (T47D and MCF-7; Fig. 1*Bii*), in which the increased *hPar1* level was inhibited by applying ICI 182,780, an E_2 antagonist (32). While 1×10^{-7} M ICI 182,780 alone had no effect on the endogenous *hPar1* level, in the presence of E_2 it completely abolished the induced *hPar1* mRNA expression in both MCF-7 and T47D cell lines (Fig. 1*Bii*). Western blot analyses verified the increase in PAR_1 protein levels following E_2 treatment (10^{-8} M &10^{-9} M, 2 h) in ER^+ MCF-7, as well as in T47D cells (data not shown), but not in MDA-231 cells, which lack ER (Fig. 1*C*). The responsiveness of the *hPar1* promoter to E_2 was shown following transient transfection of *hPar1*-driven LUC promoter and subsequent analysis of its activity. As seen in Fig. 1*D*, LUC-*hPar1* promoter activity was increased 4-fold ($P<0.005$) by E_2 treatment (2 h, 10^{-8} M). A similar increase in LUC-*hPar1* promoter activity was obtained at 10^{-9} M E_2 treatment for longer periods of incubation (*e.g.*, 6 h; data not shown). This elevated LUC-*hPar1* promoter activity was completely blocked by the E_2 inhibitor, ICI (Fig. 1*D*). MCF-7 cells treated with E_2 (representing elicited PAR_1 levels) exhibit greater sensitivity to thrombin as compared with cells prior to E_2 treatment. This is demonstrated by the Ca^{+2} flux assay performed in MCF-7 activated by thrombin before and after E_2 application. As shown in Fig. 1*E*, a marked elevation of nearly 5-fold in the Ca^{+2} response was obtained in the E_2-treated cells in thrombin concentration range analyzed (*i.e.*, 100–750 nM).

Binding properties of *hPar1*-ERE consensus motifs

To determine which of the candidate E_2-consensus sites are functional and capable of binding protein (*e.g.*, ligated ER), we prepared NEs of ER^+ MCF-7 cells. In parallel, we end-labeled the oligonucleotides representing EREs in the *hPar1* promoter corresponding to *hPar1* ERE 1, 2, and 5 (designated as P1, P2, and P5; see **Fig. 3*C***). As shown in **Fig. 2**, incubation of ^{32}P-labeled oligos with E_2 resulted in specific DNA-protein complexes. Significant binding was observed in the oligo representing C (*i.e.*, 5′-caggtcatcatgacctg-3′), the known consensus binding motif for ERE, serving as a positive control (Fig. 2, lane 4), as well as in P1 (Fig. 2, lane 8), P2 (Fig. 2, lane 10), and P5 (Fig. 2, lane 12). The binding is specific, since no binding was observed when the NE was not present in the assay (Fig. 2, lanes 1, 3), when NE of cells that do not express ER (*e.g.*, DU-145 prostate cancer cells; Fig. 2, lane 14) was applied, or prior to E_2 treatment (Fig. 2, lane 2). Significant binding was observed after E_2 treatment (Fig. 2, lanes 4, 8, 10, 12). Competition for binding between protein and DNA following E_2 treatment, in the presence of excess unlabeled oligos representing P1, P2, or P5 (Fig. 2, lanes 9, 11, 13), showed effective inhibition of the ligated ER. Mutated oligonucleotides representing the 5 ERE motifs found in the *hPar1* promoter were prepared as described in Materials and Methods. EMSA revealed that excess cold amounts ($\times$1000) of the mutated *hPar1*-EREs failed to compete with the corresponding WT oligonucleotide of each of the individual ERE site (data not shown). Mutants of P3 and P4 did not have any effect, since their labeled oligos did not bind in the first place (see below for nonfunctional ERE sites). Moreover, utilizing excess cold amounts of P1, P2, or P5 ERE oligos effectively inhibited the binding of the consensus C-ERE (Fig. 2, lanes 5, 6, 7). No binding of P1, P2, or P5 was observed prior to E_2 treatment (data not shown). No specific interaction was seen when oligos representing ERE 3 and ERE 4 (termed P3 and P4, respectively; outlined sequence shown in Fig. 3*C*) were applied, regardless of E_2 treatment (data not shown). Application of anti-ER antibodies (anti-ERα, D-12; Santa Cruz Biotechnology) to the binding assay and following E_2 treatment efficiently abrogated the binding of ER to each of the oligos tested, regardless of whether the consensus motif or the *hPar1*-representing ERE motifs were tested (Fig. 2, lanes 15, 17, 19, 21). This outcome further demonstrates that the anti-ER antibody recognizes the epitope in ER that interacts with the EREs present in the *hPar1* promoter, thereby interfering with these associations. While it is common to obtain a bandshift effect, we repeatedly observed band abrogation, which is not often obtained. Control IgG had no effect on the binding properties (Fig. 2, lane 23). This outcome strongly suggests that the 3 ERE motifs located within the *hPar1* regulatory sites are functional and capable of interacting in a sequence-specific manner with the cognate ER.

We next asked whether the E_2-responsive regions identified in the *hPar1* promoter physically interact *in*

---

or empty vector plasmids and either treated or not with 10^{-8} M E_2 for a period of 2 h. A marked up-regulation in LUC activity was obtained during this time frame at a concentration of 10^{-8} M, but not at 10^{-9} M. The specificity toward E_2 regulation is shown by application of the inhibitor, ICI. While ICI itself did not have any effect on *hPar1*-LUC activity, it potently inhibited the E_2-elicited *hPar1*-LUC activity. Luciferase activity was normalized to β-gal activity as a control for transfection efficiency. Values are means ± SD (n=6). Data are representative of ≥5 experiments. *E*) Ca^{+2} flux signaling of thrombin-treated MCF-7 cells before and after E_2 treatment. MCF-7 cells were seeded onto 96-well plates and were serum deprived for 24 h before E_2 treatment. E_2-treated cells (2 h) were loaded with Fura2AM (5 μM, 60 min) in Na-HEPES-buffered saline at pH 7.4. Cells were then treated with thrombin at the indicated concentrations and monitored every 30 s. Fluorescence was measured by a dual wavelength excitation fluorimeter at 340 and 380 nm (510 nm for emission) in a Fluro Scan Ascent SL (Thermo Electron).

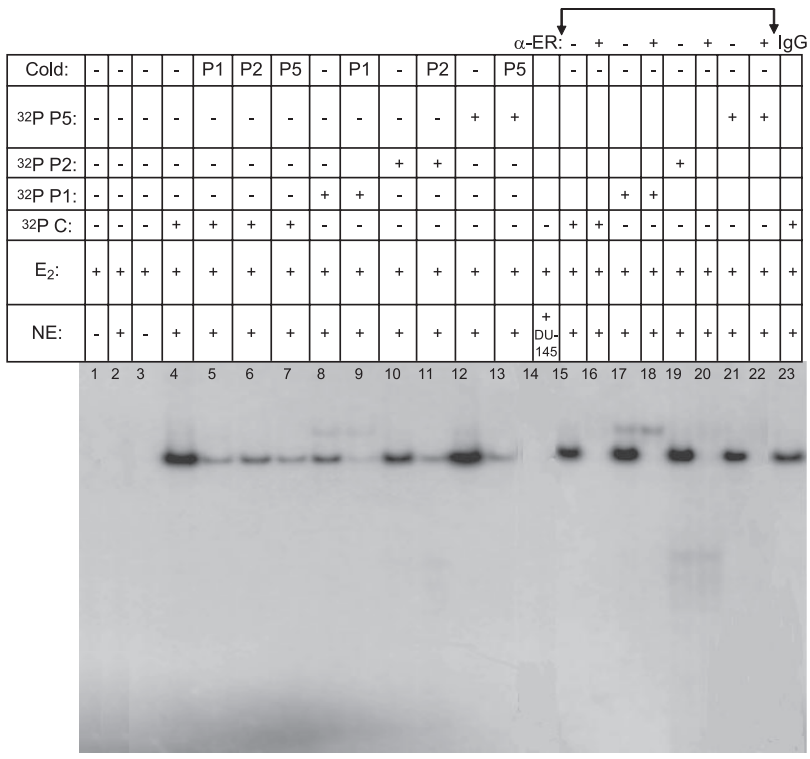

Figure 2. Identification of functional EREs in *hPar$_1$* promoter. NEs of MCF-7 cells and ^{32}P-labeled ERE oligos were used in an EMSA analysis. E_2 treatment enhanced binding of either a known ERE sequence positive control (C) or *hPar1*-ERE P1, P2, and P5 oligos (lanes 4, 8, 10, and 12, respectively) as compared with competition in the presence of excess unlabeled oligos. Competition with excess unlabeled ERE P1, P2 or P5 (lanes 5, 6, and 7, respectively) inhibited the binding of ^{32}P-labeled ERE consensus sequence oligos C (lane 4). Likewise, competition with excess unlabeled *hPar$_1$* ERE P1 oligo inhibited the binding of ^{32}P-labeled ERE P1 (lanes 8 and 9, respectively). Competition with excess unlabeled *hPar$_1$* ERE P2 oligo inhibited binding of ^{32}P-P2 oligo, while excess cold P5 inhibited the binding of ^{32}P-P5 oligo (*e.g.*, lanes 10 *vs.* 11, and 12 *vs.* 13, respectively). Control ERE showed no binding when either no NE (lanes 1, 3) or NE without E_2 treatment (lane 2) was applied. Similarly, when NE of DU-145 cells that do not express ER was used, no binding was observed (lane 14). When anti-ER antibodies were applied to the binding system, inhibition of binding of consensus (lane 15 *vs.* 16) and *hPar1*-EREs P1, P2, and P5 (lanes 17 *vs.* 18, 19 *vs.* 20, and 21 *vs.* 22, respectively) were obtained. As a control, when IgG was applied to the binding system, no effect was observed for either ^{32}P oligos C (lane 23) or ^{32}P oligos P1, P2, or P5 (data not shown). Data are representative of ≥3 experiments.

vivo with ER. ChIP analysis on MCF-7 cells was performed before and after E_2 treatment. Chromatin was isolated and immunoprecipitated with anti-ERα antibodies. DNA obtained from the immunoprecipitated chromatin was amplified utilizing 2 sets of primers directed to encompass ERE motifs within the *hPar$_1$* promoter. The signal level obtained in the noncomplexed chromatin PCR confirmed that equal amounts of DNA had been loaded. A specific increase of ≥3-fold in the presence of E_2 as compared with untreated cells was obtained. When antibody directed to an irrelevant protein (Flt-1, a cell surface receptor) or control IgG was used to immunoprecipitate the chromatin from the cell lysates (before and after E_2 treatment), minimal levels were observed, which were not affected by E_2 treatment (Fig. 3*A*). As controls, primers were planned to amplify regions outside the ERE-*hPar$_1$* motifs. These primers were directed to amplify an area located downstream to the ERE in the 5′ promoter site, as well as to recognize a site within the 3′ *hPar$_1$* gene. While both sets of primers effectively recognized the promoter cDNA construct or the 3′ region of the gene, respectively, they failed to amplify DNA obtained from the immunocomplex (Fig. 3*B*). These results further validate a direct and specific association between E_2-ligated ER and the ERE motifs found in the 5′ regulatory region of *hPar$_1$*.

E_2 induces PAR_1-associated breast cancer angiogenesis: elicited endothelial tube-forming network in 3D cultures

We previously demonstrated that activation of PAR_1 markedly augments the expression and function of VEGF mRNA splice forms, as determined by *in vitro* assays for endothelial tube alignment (24). We examined whether treatment with E_2 (*i.e.*, 10^{-8} M, 2 h) of either MCF-7 or T47D cells expressing ER is capable of eliciting the expression of functional VEGF. Indeed, as shown in **Fig. 4*A***, E_2 treatment (*i.e.*, 2 h) before and after PAR_1 activation (*i.e.*, 6 h) enhanced the levels of $VEGF_{165}$.

To determine whether the increased levels of VEGF mRNA and protein induced by *hPar$_1$* gene correspond to increased levels of functional protein, we collected CM from either untreated or E_2-treated MCF-7 cells, before and after PAR_1 activation. To establish how much VEGF is produced and secreted, VEGF-CM was quantitated by ELISA. In CM (up to 30 h) derived from control cells (no PAR_1 expression), there was no significant VEGF release (<18 pg/ml). In 6- to 8-h CM derived from MCF-7 cells following E_2 treatment and PAR_1 activation, VEGF levels were 1112 ± 18 pg/ml ($P<0.01$), compared with 311.2 ± 22 pg/ml in nonactivated MCF-7 cells treated with E_2. Thirty-hour CM from nonactivated MCF-7 cells treated with E_2 contained 989 ± 112.7 pg/ml VEGF; on PAR_1 activation, VEGF release was increased to 3996.3 ± 221.4 pg/ml ($P<0.005$). Levels of VEGF in the CM of nonactivated MDA-435 were 1521 ± 112.8 pg/ml and following PAR_1 activation increased to 4996.3 ± pg/ml ($P<0.05$). We employed an endothelial tube-forming assay to assess the VEGF activity present in the CM. BAECs were embedded in a 3D collagen (type I) mesh, and the extent of tube-forming network was evaluated after application of the various CMs (24). Although low

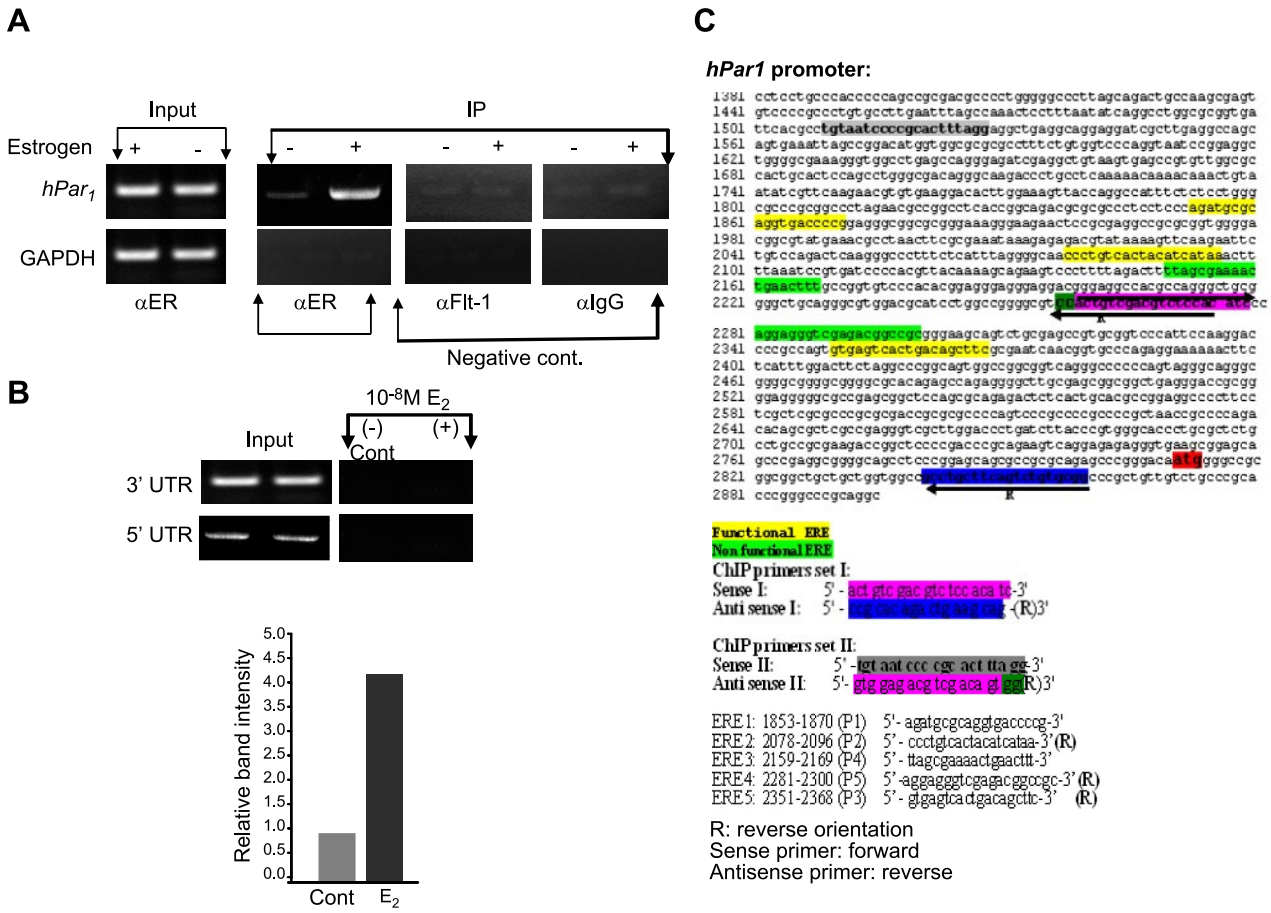

Figure 3. ChIP assay to demonstrate the *in vivo* interaction between ER and the *hPar1*-ER consensus site. *A*) DNA fragments immunoprecipitated with the indicated antibodies were purified, and the regions containing the ERE proposed sites were amplified by PCR. An equal amount (input) of DNA was applied. PCR products generated using either $hPar_1$ promoter primers or GAPDH primers to amplify from immunoprecipitated DNA before (−) and after (+) E_2 treatment of MCF-7. GAPDH primers, control IgG, and nonrelative (α Flt-1) antibody were used as controls for nonspecific immunocomplexes. Results are representative of ≥3 independent experiments. *B*) As controls, a set of primers was designed to amplify regions outside the ERE motifs. One set of controls was designed to amplify a region located downstream to the ERE in the 5′ promoter site (5 UTR). The second set was designed to recognize a region in the 3′ end of $hPar_1$. Neither of the primers gave a product when amplifying DNA from the immunocomplex. These controls emphasize the specificity of the $hPar_1$-ERE located at the 5′ regulatory region of the gene. *C*) 5′ flanking sequences of PAR_1 promoter and proposed *ERE* motifs are shown. Functional and nonfunctional EREs are highlighted, as are the sequences of the 2 sets of primers used. Data are representative of 3 experiments.

vascular branching activity was obtained with untreated control CM, with or without thrombin treatment, a more complex network was observed following activation of PAR_1 that was overexpressed by E_2-treatment in the ER-expressing MCF-7 cells (Fig. 4*Bi*). One should keep in mind that VEGF alone is a target for ER transcriptional regulation (33). EREs are found within the VEGF promoter; therefore, E2 treatment alone may induce VEGF levels. However, the specificity for $hPar_1$ enhanced VEGF in our experimental system was demonstrated by applying CM collected from cells infected with an siRNA-$hPar_1$ lentiviral vector, in either MDA-435 metastatic breast cancer cells that overexpress $hPar_1$ (Fig. 4*BiVIII*) or in MCF-7 cells that were treated with E_2 (Fig. 4*BiIV*). To show that activation of PAR_1 induces VEGF, application of anti-VEGF-neutralizing Abs C20 (Santa Cruz Biotechnology) was carried out, leading to the abrogation of tube network formation (Fig. 4*BiVI*). These data demonstrate that E_2 treatment of ER-expressing MCF-7 cells elevates PAR_1 expression to generate functional angiogenesis.

Functional consequences of PAR_1 expression in clinical samples of breast carcinoma

The molecular characterization of breast cancer subtypes has led to significant progress in treating this type of malignancy. Advancing tumor categorization and identifying cellular imprints to accompany histopathological assessment may provide cellular targets for therapy, as well as effective vehicles to evaluate the response to a given treatment. Immunohistochemical analyses were used to evaluate the profile of PAR_1 overexpression in clinically obtained breast cancer biopsy specimens. A tissue microarray obtained from an established cohort of 299 women diagnosed (**Table 1**) with invasive breast carcinoma was immunostained for

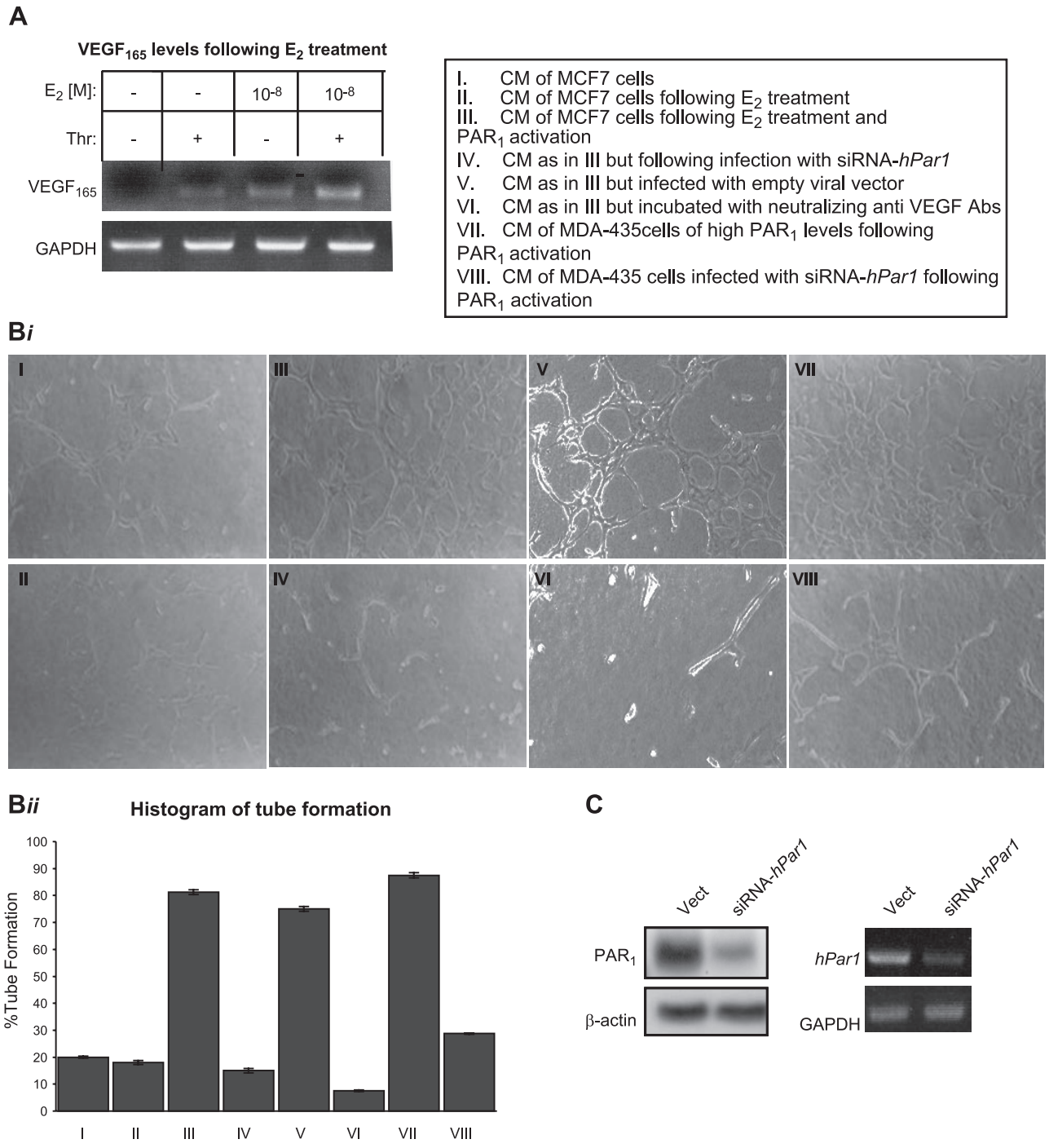

Figure 4. E_2 treatment of MCF-7 cells elicits PAR_1-induced functional VEGF. *A*) Semiquantitative RT-PCR for $VEGF_{165}$. Analyses of RNA isolated from MCF-7 cells demonstrate increased levels of $VEGF_{165}$ following E_2 treatment (*i.e.*, 2 h, 10^{-8} M) alone, and long-term PAR_1 activation (6 h) by thrombin or the ligand-activating peptide, TFLLRNPNDK (data not shown). No expression of $VEGF_{165}$ is seen in MCF-7 cells prior to E_2 treatment. *Bi*) Endothelial cell tube-forming assay. CM from either MCF-7 cells before and after E_2 treatment or MDA-435 expressing high PAR_1 levels increases the complexity of cell tube formation. Cultures of endothelial cells in a 3D collagen type I matrix were grown with CM from nonmetastatic MCF-7 cells expressing very little or no *hPar1*, before and after E_2 treatment and PAR_1 activation (*I–III*), or activated MDA-435 cells (*VII, VIII*). The importance of PAR_1 in the process is demonstrated following silencing of *hPar1* after infection with siRNA-*hPar1* either in MCF-7 cells (*IV, V*) or MDA-435 cells (*VIII*). The effect of VEGF is shown by incubating CM from E_2 treatment as well as PAR_1 activation with neutralizing anti-VEGF Abs C20 (*VI*; Santa Cruz Biotechnology). *Bii*) Morphometric analysis used to evaluate tube formation was performed as explained in Materials and Methods. Briefly, each well in a given plate (per treatment) was independently evaluated by 2 investigators (M.J. and R.B.). Discrepancies were resolved by simultaneous reexamination of the wells by both investigators using a double-headed microscope. The microscope was calibrated with a micrometer slide before each measurement. Ten fused cells/field were selected, and ≥50 fused cells/treatment case were assessed. Four microscopic fields were screened. Error bars = means ± SD; difference between groups was determined by χ^2 test. Data are representative of 4 independent experiments performed in triplicate. *C*) Silencing of *hPar1* by siRNA construct. Infection of siRNA-*hPar1* in MDA-435 cells leads to the inhibition of PAR_1 protein and RNA. These data are representative of ≥3 experiments.

TABLE 1. *Characteristics of study population (n=299 subjects): clinical and pathological aspects*

Parameter	Value
Criteria	
Age (yr)	49 (20–82)
Tumor size (cm)	2 (0.2–9)
Tumor type [n (%)]	
IDC	220 (73.5)
ILC	33 (11)
IDC + ILC	13 (4.3)
DCIS	9 (3.0)
DCIS + microinvasion	14 (4.6)
Mucinous	3 (1.0)
Medullary	7 (2.3)
Lymph node status [n (%)]	
LN-negative	159 (53.1)
LN-positive	120 (40.1)
Grade [n (%)]	
1–2	161 (54.5)
3	134 (45.4)
Total valid	295
ER [n (%)]	
Negative	105 (37.2)
Positive	177 (62.7)
Total valid	282
PR [n (%)]	
Negative	235 (84.2)
Positive	44 (15.7)
Total valid	279
TN [n (%)]	95 (34.79)
Total valid	273

Values are median and range for criteria; number of cases and percentage for all other parameters. DCIS, ductal carcinoma *in situ*; IDC, invasive ductal carcinoma; ILC, invasive lobular carcinoma; TN, triple negative.

PAR_1 (**Fig. 5**) and ER/PR (data not shown). While the frequency of ER positivity was 62% (176 tumors), and PR was expressed in 44 (15%) tumors, PAR_1 expression was found in 76% of all the tumors. No PAR_1 expression was detected in any of the 5 control specimens of nonmalignant breast tissues (Fig. 5, representative control staining).

χ^2 analysis of DFS of the ER^+ patients (5 yr retrospectively) among the tissue microarray cohort of patients that overexpress or do not overexpress PAR_1 showed the following outcome. A markedly significant (P=0.006) difference in the DFS in women that overexpress both ER^+ and PAR_1 represented a distinctly shorter DFS (median not reached) compared with patients who were ER^+ but negative for PAR_1 (Fig. 5*B*). Likewise, a shorter OS was observed in ER^+ and $PAR_1{}^+$ patients, compared with ER^+ and $PAR_1{}^-$ (P=0.021) patients. These observations strengthen the concept that PAR_1 may account for part of a highly malignant gene signature in breast carcinoma.

DISCUSSION

With the goal of gaining mechanistic insights into PAR_1 and E_2 action in the etiology of breast cancer progression, we examined functional consequences of PAR_1 expression in clinical tissue microarray settings and biochemically characterized E_2 regulation of *hPar1* expression. An ongoing challenge is to identify molecular means to assist in evaluating the degree of response to a given therapy. Five-year retrospective analyses of ER^+ patients that express PAR_1 resulted in a significantly shorter DFS and OS compared with ER^+ but $PAR_1{}^-$ patients. This could aid in optimizing our approach to personalized care whereby genetic print/s may improve the prediction of the course of disease and response to treatment. Indeed, gene signature might complement the traditional pathological assessment in evaluating tumor behavior. Similarly, Oncotype Dx, a gene profile that has been recently developed for women with hormone receptor-positive disease, is a good example of such refinement and is part of an oncologist's practice today (34). Accordingly, while a low score is consistent with hormone therapy, a high score indicates that the addition of treatment such as chemotherapy may be required. The presence of PAR_1 may tilt the score or stand on its own when making a decision on treatment. In addition, despite early detection that is more common today, there are still small tumors (*e.g.*, early detection) that can cause death. In these tumors, newly emerging biological biomarkers may greatly assist in making a treatment decision.

The regulatory sequence of *hPar1* has been cloned (35), enabling the identification of specific transcription factors (*i.e.*, Sp1, *Egr-1*), as well as tumor suppressor genes (*i.e.*, AP_2 and p53), as potent regulators of the *hPar1* gene (27, 29, 36). Yet the molecular pathway responsible for enhanced *hPar1* overexpression in developing tumors as compared with normal tissues of the same origin remains poorly understood.

Transcriptional regulation plays a central role in *hPar1* tumor-associated gene overexpression. We have demonstrated that *Egr-1* acts at the transcriptional level to noticeably induce *hPar1* gene levels in prostate cancer (27). Here p53, a nuclear transcription factor and a well-studied tumor suppressor gene, was also shown as a regulator of *hPar1* gene expression and function (29). While an inverse correlation exists between WT p53 expression and *hPar1*, the mutant p53 forms, representing either loss of p53 or impaired function, directly correlate with *hPar1* overexpression in cancer (29). Likewise, Tellez *et al.* (36) demonstrated an inverse correlation between the expression of activator protein-2α (AP-2) and the overexpression of PAR_1 in metastatic melanoma. In contrast, a direct correlation has been established between the expression of specificity protein 1 (Sp1) and aggressive melanoma (36). Altogether, these observations strengthen the notion that specific transcription factors and tumor suppressors may delicately regulate the overexpression of the *hPar1* gene in a given cancer context.

Promoter analyses have identified the functional ERE regions in the *hPar1* regulatory region by employing EMSA examinations, which point to the regions corresponding to P1, P2, and P5 capable of specifically

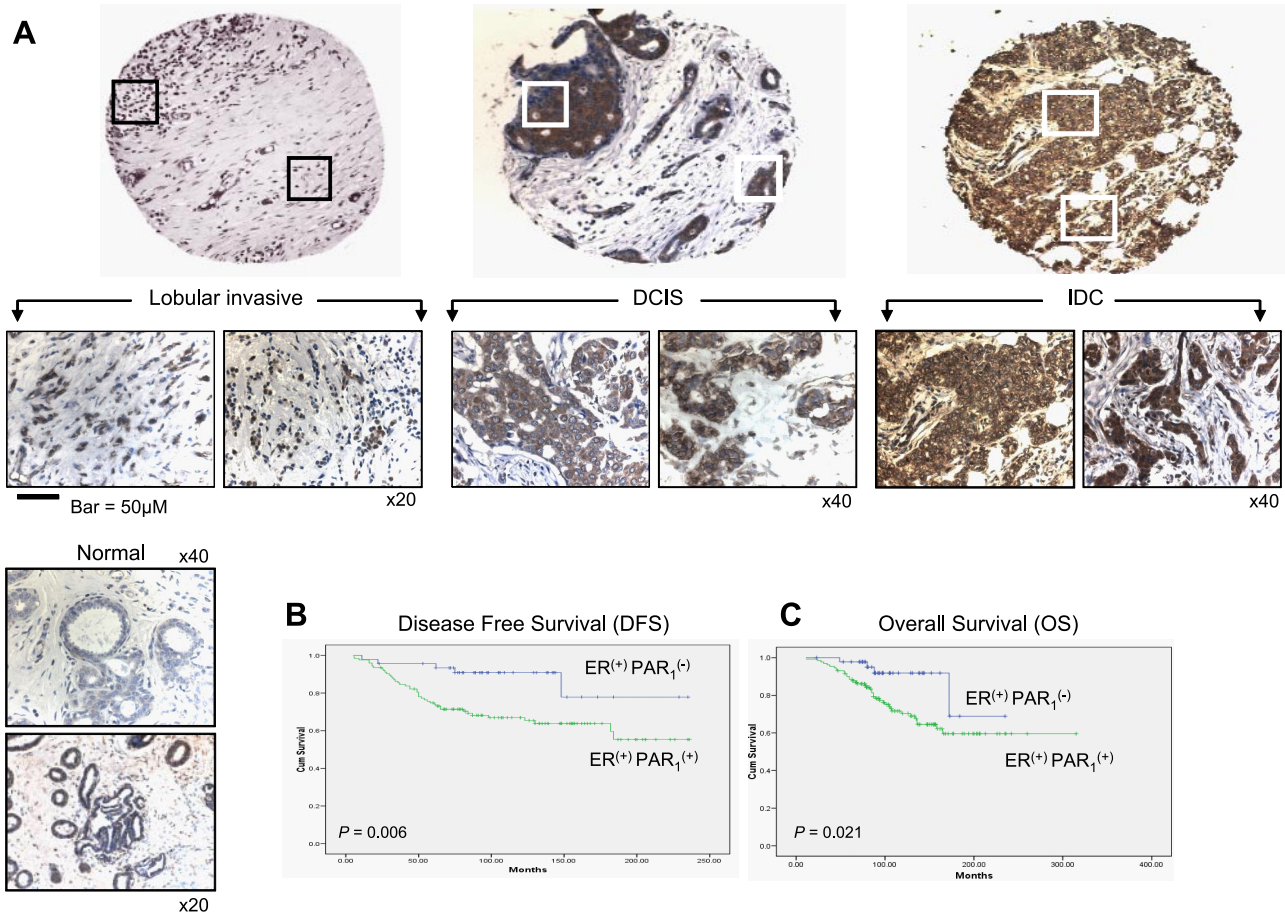

Figure 5. Immunohistological staining of PAR_1 in breast cancer tissue microarray. *A*) Representative images of positive PAR_1 immunostaining in breast carcinoma tissue microarray (left, invasive lobular carcinoma; middle, ductal carcinoma *in situ* [DCIS]; right, invasive ductal carcinoma [IDC]), as well as negative staining on sections of normal breast tissues. Histological evaluation was carried out utilizing anatomical compartments of an ocular micrometer. Slide review was independently performed by an expert pathologist (B.M.). The microscope was calibrated with a micrometer slide before each measurement. All measurements were performed on the monitor screen using a ×40 objective. On examining the sections, fields representing tumor cells from the most cellular area at the center of the tumor were selected. Necrotic and inflammatory areas were avoided. Five microscopic fields were screened. Ten cells/field were selected, and ≥50 cells/tumor case were assessed. Definition of a tumor as PAR_1^+ was based on ≥25% staining of tumor cells (cutoff point of 25%). Immunostained tumor cells were chosen on the basis of an initial overview of the cases to improve signal-to-noise ratios. Discrepancies were resolved by simultaneous reexamination of the slides by both investigators (B.M. and Z.S.) using a double-headed microscope. Histological scoring was based on the following: +1, <25% positive cells (weak positive); +2, between 25 and 75% positive cells (moderate); +3, >75% positive cells (strong). All controls were negative (0–5% positive cells). Extent of expression classified by score (1–3), number of positive cells/field (x=5). *B*) Immunohistological staining of PAR_1 in breast cancer tissue microarray. Retrospective (5-yr) analysis of ER^+ tumors in women represented by the tissue microarray revealed that patients that express both ER and PAR_1 exhibit a significantly shorter DFS (P=0.006; median not reached) compared with ER^+ but PAR_1^- patients. *C*) OS of women according to ER and PAR_1 levels. Retrospective (5-yr) analysis of ER^+ tumors in women represented by the tissue microarray revealed a significantly shorter OS (P=0.021; median not reached) compared with ER^+ but PAR_1^- women.

associating with ER present within the NEs in the assay. ChIP analysis confirmed physical *in vivo* association occurring between the functional ERE motifs and ER. It remains to be determined whether the observed E_2 stimulation of $hPar_1$ may be attributed in part to interplay between the ER and the $hPar_1$-inducing transcription factors found to regulate $hPar_1$ transcriptional activity.

PAR_1 is tightly associated with breast cancer tumorigenesis, as demonstrated by the orthotopic inoculation of cells expressing $hPar_1$ into mouse mammary glands *in vivo*. Large and highly vascularized tumors were generated when MCF-7 cells were genetically engineered to overexpress either WT $hPar_1$ or *Y397Z hPar1*, with persistent signaling. In contrast, cells overexpressing the truncated form of $hPar_1$, which lacks the cytoplasmic tail, developed small or no tumors, similar to cells expressing empty vector or control untreated cells (25). This outcome highlights the role of signaling in PAR_1-induced breast cancer growth and development. Indeed, antibody-array membranes revealed essential $hPar_1$ partners, including Etk/Bmx and Shc. The hierarchy of binding, as well as the minimal binding region in PAR_1 C-tail, was established, rendering this region a potential platform for therapeutic vehicles in breast cancer.

Here we have demonstrated E_2 responsiveness of the *hPar1* gene promoter and have found that exposure to physiological concentrations of E_2 induces *hPar1* expression in breast carcinoma cells. The E_2 effect on *hPar1* expression occurred in an ER^+, but not in an ER^- breast carcinoma cell line, and was inhibited by the anti-E_2 ICI 182,780, known to block responses mediated through ER signaling (32). These data indicate that the classic ER pathway is involved in transcriptional activation of *hPar1* rather than numerous alternative mechanisms of E_2-regulated cell responses (34, 37, 38). Tamoxifen, the most widely used anti-E_2 in endocrine therapy of breast cancer, plays a dual role. It can act as an antagonist at a high concentration, inhibiting E_2-induced *hPar1* levels, whereas at physiological concentrations it acts as an agonist for the ER-inducing levels of *hPar1* (unpublished results).

While we describe here a canonical mode of E_2-bound ER transcriptional activity (*via* binding to ERE motifs present on the *hPar1* promoter), noncanonical E_2 activation has also been described. ER can interact with other transcription factors, through a process referred to as transcription factor crosstalk. In this case, ER can modulate the activities of other transcription factors such as activator protein (AP)-1, nuclear factor-κB (NF-κB), or SP-1, by stabilizing their DNA binding and/or recruiting coactivators to the complex (39–41). Another mechanism by which E_2 and ER affect gene expression has been termed the nongenomic pathway. In this pathway, E_2 binds to the ER localized outside the cell nucleus (in the cytoplasm or membrane). This, in turn, activates signal transduction pathways in the cytosol, for example, MAPK signaling. The AP-1 transcription factor, which acts through GC-rich regions in the promoter, affects many growth factor receptors, including IGF-1R, erbB 2, and EGFR, leading to MAPK activation, which acts to phosphorylate ER (Ser118) or ER coactivator phosphorylation, thereby leading to increased ER activity (42, 43). PAR_1, once expressed, is known to activate the MAPK pathway, hence contributing to improved ER transcriptional activities. AP-binding motifs are in fact present in 4 different locations throughout the *hPar1* promoter. It is possible that once PAR_1 is expressed by the canonical ERE pathway, other mechanisms may also be involved. These include transcription-factor crosstalk with AP-1, or *via* the nongenomic activation signaling of the MAPK pathway, which will enhance and improve ER transcriptional activity (44–46).

E_2-induced *hPar1* could be particularly important in the initial stages of breast cancer, when the majority of breast tumors are reportedly ER^+ (47, 48). Overexpression of *hPar1* has also been observed in cases of ER^-, more violent tumors, whereby its level is controlled by selective transcription-factors that come into view as critical regulators. What these specific transcription factors that regulate *hPar1* overexpression in breast cancer are is yet unknown. These aggressive tumors that are E_2 independent are resistant to traditional anti-E_2 therapy. In these tumors, high *hPar1* levels, at least in part, account for the more aggressive phenotype and poor prognosis. Consequently, while targeted therapeutics toward PAR_1 [*e.g.*, SCH 530348, an oral anti-PAR_1 antagonist under phase 3 clinical evaluation in patients with atherothrombotic disease (48, 49), or pepducin, which inhibits PAR_1 intracellular function and the cell-penetrating inhibitory peptides, pepducins] are not part of the oncologists' list of protocols, the presence of PAR_1 identifies patients who may require chemotherapy in addition to hormone treatment. In addition, it may provide the basis for broadening an oncologist's therapeutic procedures. These studies provide a guide to treatment decisions on individual-based care. Furthermore, these inhibitors may be considered for future therapeutic modality in breast cancer. FJ

This work was supported in part by funds from the Israel Scientific Foundation (ISF) and the Ministry of Industry and Trade, Nofar project (to R.B.).

REFERENCES

1. Di Cosimo, S., and Baselga, J. (2010) Management of breast cancer with targeted agents: importance of heterogeneity. *Nat. Rev. Clin. Oncol.* **7,** 139–147
2. Jemal, A., Siegel, R., Ward, E., Hao, Y., Xu, J., and Thun, M. J. (2009) Cancer statistics. *CA Cancer J. Clin.* **59,** 225–249
3. Brisken, C., and O'Malley, B. (2010) Hormone action in the mammary gland. *Cold Spring Harbor Perspect. Biol.* **2**(12): a003178,
4. Daniel, C. W., Silberstein, G. B., and Strickland, P. (1987) Direct action of 17 beta-estradiol on mouse mammary ducts analyzed by sustained release implants and steroid autoradiography. *Cancer Res.* **47,** 6052–6057
5. Silberstein, G. B., Van Horn, K., Shyamala, G., and Daniel, C. W. (1994) Essential role of endogenous estrogen in directly stimulating mammary growth demonstrated by implants containing pure antiestrogens. *Endocrinology* **134,** 84–90
6. Lippman, M. E., and Bolan, G. O. (1975) Estrogen-responsive human breast cancer in long-term tissue culture. *Nature* **256,** 592–593
7. Xu, J., Wu, R. C., and O'Malley, B. W. (2009) Normal and cancer-related functions of the p160 steroid receptor co-activator (SRC) family. *Nat. Rev. Cancer* **9,** 615–630
8. Clarke, R. B., Howell, A., Potten, C. S., and Anderson, E. (1997) Dissociation between steroid receptor expression and cell proliferation in the human breast. *Cancer Res.* **57,** 4987–4991
9. McKenna, N. J., Lanz, R. B., and O'Malley, B. W. (1999) Nuclear receptor coregulators: cellular and molecular biology. *Endocr. Rev.* **20,** 321–344
10. McKenna, N. J., and O'Malley, B. W. (2002) Minireview: nuclear receptor coactivators—an update. *Endocrinology* **143,** 2461–2465
11. Charpentier, A. H., Bednarek, A. K., Daniel, R.L., Hawkins, K. A., Laflin, K. J., Gaddis, S., MacLeod, M. C., and Aldaz, C. M. (2000) Effects of estrogen on global gene expression: identification of novel targets of estrogen action. *Cancer Res.* **60,** 5977–5983
12. Levin, E. R. (2003) Bidirectional signaling between the estrogen receptor and the epidermal growth factor receptor. *Mol. Endocr.* **17,** 309–317
13. Fan, P., Wang, J., Santen, R. J., and Yue, W. (2007) Long-term treatment with tamoxifen facilitates translocation of estrogen receptor alpha out of the nucleus and enhances its interaction with EGFR in MCF-7 breast cancer cells. *Cancer Res.* **67,** 1352–1360
14. Song, R. X., Fan, P., Yue, W., Chen, Y., and Santen, R. J. (2006) Role of receptor complexes in the extranuclear actions of estrogen receptor alpha in breast cancer. *Endocr. Relat. Cancer* **13**(Suppl. 1), S3–S13

15. Wu, R. C., Smith, C. L., and O'Malley, B. W. (2005) Transcriptional regulation by steroid receptor coactivator phosphorylation. *Endocr. Rev.* **26,** 393–399
16. Vu, T. K., Hung, D. T., Wheaton, V. I., and Coughlin, S. R. (1991) Molecular cloning of a functional thrombin receptor reveals a novel proteolytic mechanism of receptor activation. *Cell* **64,** 1057–1068
17. Coughlin, S. R. (2000) Thrombin signalling and protease-activated receptors. *Nature* **407,** 258–264
18. Rickles, F. R., and Edwards, R. L. (1983) Activation of blood coagulation in cancer: Trousseau's syndrome revisited. *Blood* **62,** 14–31
19. Palumbo, J. S., Kombrinck, K. W., Drew, A. F., Grimes, T. S., Kiser, J. H., Degen, J. L., and Bugge, T. H. (2000) Fibrinogen is an important determinant of the metastatic potential of circulating tumor cells. *Blood* **96,** 3302–3309
20. Riewald, M., Kravchenko, V. V., Petrovan, R. J., O'Brien, P. J., Brass, L. F., Ulevitch, R. J., and Ruf, W. (2001) Gene induction by coagulation factor Xa is mediated by activation of protease-activated receptor 1. *Blood* **97,** 3109–3116
21. Even-Ram, S., Uziely, B., Cohen, P., Grisaru-Granovsky, S., Maoz, M., Ginzburg, Y., Reich, R., Vlodavsky, I., and Bar-Shavit, R. (1998) Thrombin receptor overexpression in malignant and physiological invasion processes. *Nat. Med.* **4,** 909–914
22. Booden, M. A., Eckert, L. B., Der, C. J., and Trejo, J. (2004) Persistent signaling by dysregulated thrombin receptor trafficking promotes breast carcinoma cell invasion. *Mol. Cell. Biol.* **24,** 1990–1999
23. Yang, E., Boire, A., Agarwal, A., Nguyen, N., O'Callaghan, K., Tu, P., Kuliopulos, A., and Covic, L. (2009) Blockade of PAR1 signaling with cell-penetrating pepducins inhibits Akt survival pathways in breast cancer cells and suppresses tumor survival and metastasis. *Cancer Res.* **69,** 6223–6231
24. Yin, Y. J., Salah, Z., Maoz, M., Ram, S. C., Ochayon, S., Neufeld, G., Katzav, S., and Bar-Shavit, R. (2003) Oncogenic transformation induces tumor angiogenesis: a role for PAR1 activation. *FASEB J.* **17,** 63–174
25. Cohen, I., Maoz, M., Turm, H., Grisaru-Granovsky, S., Maly, B., Uziely, B., Weiss, E., Abramovitch, R., Gross, E., Barzilay, O., Qiu, Y., and Bar-Shavit, R. (2010) Etk/Bmx regulates proteinase-activated-receptor1 (PAR1) in breast cancer invasion: signaling partners, hierarchy and physiological significance. *PLoS ONE* **5,** e11135
26. Miao, H. Q., Ornitz, D. M., Aingorn, E., Ben-Sasson, S. A., and Vlodavsky, I. (1997) Modulation of fibroblast growth factor-2 receptor binding, dimerization, signaling, and angiogenic activity by a synthetic heparin-mimicking polyanionic compound. *J. Clin. Invest.* **99,** 1565–1575
27. Salah, Z., Maoz, M., Pizov, G., and Bar-Shavit, R. (2007) Transcriptional regulation of human protease-activated receptor 1: a role for the early growth response-1 protein in prostate cancer. *Cancer Res.* **67,** 9835–9843
28. Andrews, N. C., and Faller, D. V. (1991) A rapid micropreparation technique for extraction of DNA-binding proteins from limiting numbers of mammalian cells. *Nucleic Acids Res.* **19,** 2499
29. Salah, Z., Haupt, S., Maoz, M., Baraz, L., Rotter, V., Peretz, T., Haupt, Y., and Bar-Shavit, R. (2008) p53 controls *hPar1* function and expression. *Oncogene* **27,** 6866–6874
30. Kononen, J., Bubendorf, L., Kallioniemi, A., Bärlund, M., Schraml, P., Leighton, S., Torhorst, J., Mihatsch, M. J., Sauter, G., and Kallioniemi, O. P. (1998) Tissue microarrays for high-throughput molecular profiling of tumor specimens. *Nat. Med.* **4,** 844–847
31. Hoos, A., Urist, M. J., Stojadinovic, A., Mastorides, S., Dudas, M. E., Leung, D. H., Kuo, D., Brennan, M. F., Lewis, J. J., and Cordon-Cardo, C. (2001) Validation of tissue microarrays for immunohistochemical profiling of cancer specimens using the example of human fibroblastic tumors. *Am. J. Pathol.* **158,** 1245–1251
32. Wakeling, A. E. (1992) Steroid antagonists as nuclear receptor blockers. *Cancer Surv.* **14,** 71–85
33. Applanat, M. P., Buteau-Lozano, H., Herve, M. A., and Corpet, A. (2008) Vascular endothelial growth factor is a target gene for estrogen receptor and contributes to breast cancer progression. *Adv. Exp. Med. Biol.* **617,** 437–444
34. Paik, S., Shak, S., Tang, G., Kim, C., Baker, J., Cronin, M., Baehner, F. L., Walker, M. G., Watson, D., Park, T., Hiller, W., Fisher, E. R., Wickerham, D. L., Bryant, J., and Wolmark, N. (2004) A multigene assay to predict recurrence of tamoxifen-treated, node-negative breast cancer. *N. Engl. J. Med.* **351,** 2817–2826
35. Li, F., Baykal, D., Horaist, C., Yan, C. N., Carr, B. N., Rao, G. N., and Runge, M. S. (1996) Cloning and identification of regulatory sequences of the human thrombin receptor gene. *J. Biol. Chem.* **271,** 26320–26328
36. Tellez, C., McCarty, M., Ruiz, M., and Bar-Eli, M. (2003) Loss of activator protein-2alpha results in overexpression of protease-activated receptor-1 and correlates with the malignant phenotype of human melanoma. *J. Biol. Chem.* **278,** 46632–46642
37. Creighton, C. J., Massarweh, S., Huang, S., Tsimelzon, A., Hilsenbeck, S. G., Osborne, C. K., Shou, J., Malorni, L., and Schiff, R. (2008) Development of resistance to targeted therapies transforms the clinically associated molecular profile subtype of breast tumor xenografts. *Cancer Res.* **68,** 7493–7501
38. McDonnell, D. P., and Wardell, S. E. (2010) The molecular mechanisms underlying the pharmacological actions of ER modulators: implications for new drug discovery in breast cancer. *Curr. Opin. Pharmacol.* **10,** 620–628
39. Kushner, P. J., Agard, D. A., Greene, G. L., Scanlan, T. S., Shiau, A. K., Uht, R. M., and Webb, P. (2000) Estrogen receptor pathways to AP-1. *J. Steroid Biochem. Mol. Biol.* **74,** 311–317
40. Wang, W., Dong, L., Saville, B., and Safe, S. (1999) Transcriptional activation of E2F1 gene expression by 17 beta-estradiol in MCF-7 cells is regulated by NF-Y-Sp1/estrogen receptor interactions. *Mol. Endocrinol.* **8,** 1373–1387
41. Stein, B., and Yang, M. X. (1995) Repression of the interleukin-6 promoter by estrogen receptor is mediated by NF-kappa B and C/EBP beta. *Mol. Cell. Biol.* **15,** 4971–4979
42. Kato, S., Endoh, H., Masuhiro, Y., Kitamoto, T., Uchiyama, S., Sasaki, H., Masushige, S., Gotoh, Y., Nishida, E., Kawashima, H., Metzger, D., and Chambon, P. (1995) Activation of the estrogen receptor through phosphorylation by mitogen-activated protein kinase. *Science* **270,** 1491–1494
43. DeNardo, D. G., Kim, H. T., Hilsenbeck, S., Cuba, V., Tsimelzon, A., and Brown, P. H. (2005) Global gene expression analysis of estrogen receptor transcription factor cross talk in breast cancer: identification of estrogen-induced/activator protein-1-dependent genes. *Mol. Endocrinol.* **19,** 362–378
44. Morton, S., Davis, R. J., McLaren, A., and Cohen, P. (2003) A reinvestigation of the multisite phosphorylation of the transcription factor c-Jun. *EMBO J.* **22,** 3876–3886
45. Cascio, S., Bartella, V., Garofalo, C., Russo, A., Giordano, A., and Surmacz, E. (2007) Insulin-like growth factor 1 differentially regulates estrogen receptor-dependent transcription at estrogen response element and AP-1 sites in breast cancer cells. *J. Biol. Chem.* **282,** 3498–3506
46. Schiff, R., and Osborne, C. K. (2005) Endocrinology and hormone therapy in breast cancer: new insight into estrogen receptor-alpha function and its implication for endocrine therapy resistance in breast cancer. *Breast Cancer Res.* **7,** 205–211
47. Osborne, C. K. (1998) Steroid hormone receptors in breast cancer management. *Breast Cancer Res. Treat.* **51,** 227–238
48. Becker, R. C., Moliterno, D. J., Jennings, L. K., Pieper, K. S., Pei, J., Niederman, A., Ziada, K. M., Berman, G., Strony, J., Joseph, D., Mahaffey, K. W., Van de Werf, F., Veltri, E., and Harrington, R. A. (2009) Safety and tolerability of SCH 530348 in patients undergoing non-urgent percutaneous coronary intervention: a randomized, double-blind, placebo-controlled phase II study. *Lancet* **373,** 919–928
49. White, H. D. (2011) Oral antiplatelet therapy for atherothrombotic disease: current evidence and new directions. *Am. Heart J.* **161,** 450–461

Received for publication September 8, 2011.
Accepted for publication January 17, 2012.